

Quasiparticle density of states of $\text{Bi}_2\text{Sr}_2\text{CaCu}_2\text{O}_{8+\delta}$ single crystals probed using tunneling spectroscopy in the 30–50 mK temperature range in high magnetic fields

S. I. Vedenev^{1,2} and D. K. Maude¹¹*Grenoble High Magnetic Field Laboratory, Centre National de la Recherche Scientifique, B.P. 166, F-38042 Grenoble Cedex 9, France*²*P.N. Lebedev Physical Institute, Russian Academy of Sciences, 119991 Moscow, Russia*

(Received 8 April 2004; revised manuscript received 28 July 2005; published 25 October 2005)

Break-junction tunneling spectroscopy at temperatures 30–50 mK in high magnetic field is used to directly probe the quasiparticle density of states within the energy gap in a single crystal Bi2212 high- T_c superconductor. The measured tunneling conductances $dI/dV(V)$ in the subgap region have a zero flat region with no evidence for a linear increase of the density of states with voltage. A number of tunnel break junctions exhibited $dI/dV(V)$ curves with a second energy gap structure at the average magnitude $2\Delta_{p-p}/e=13$ mV. Our data cannot be explained by either a pure s pairing or a pure $d_{x^2-y^2}$ pairing.

DOI: 10.1103/PhysRevB.72.144519

PACS number(s): 74.72.Hs, 74.50.+r

I. INTRODUCTION

A careful investigation of the density of states (DOS) for quasiparticle excitations in high- T_c copper oxide superconductors is essential for the understanding of the mechanism responsible for superconductivity. Tunneling spectroscopy has played an important role in verifying BCS theory in conventional superconductors. The conductance of a tunnel junction is directly proportional to the quasiparticle density of states. The fine structure found in the tunneling conductance at voltages above the energy gap is a direct proof that the electron-phonon interaction is the coupling mechanism for superconductivity in conventional superconductors. It is widely accepted that the high- T_c superconductors (HTS) have $d_{x^2-y^2}$ symmetry of the order parameter. Among the HTS, $\text{Bi}_2\text{Sr}_2\text{CaCu}_2\text{O}_{8+d}$ (Bi2212) has often been studied by the tunneling method. Although the tunneling characteristics obtained with Bi2212 single crystals show features related to the superconducting energy gap, the shape of the tunneling conductance dI/dV vs V is far from the ideal BCS density of states. The conductance curves reveal a strong broadening of the superconducting-gap structure, with a nonzero contribution at zero voltage and a linear increase in the subgap region (cusplike feature) (see, e.g., Refs. 1 and 2). In addition, an unusual feature frequently observed in the tunneling data of Bi2212 is the “dip-hump” structure beyond the gap edge which is close to the resonant spin excitation energy.³

In superconducting tunnel junctions, the difference between d - and s -wave symmetry leads to a significant change in the current-voltage [$I(V)$] characteristics. For an intrinsic unshunted s -wave superconductor-insulator-superconductor (SIS) junction, the zero-bias conductance should be exponentially small at low temperatures (especially in case of superconductors with high T_c). In contrast, if the order parameter has nodes and $d_{x^2-y^2}$ symmetry, the $I(V)$ characteristics of the d -wave SIS junction in the vicinity of the zero bias should have a finite slope and thus a nonzero conductance at zero voltage (see, e.g., Ref. 1). Experimental tunneling characteristics of d -wave SIS junctions do not agree with the theoretical predictions. Won and Maki⁴ found that at low temperatures the subgap tunneling conductance dI/dV

should increase almost quadratically with V . Whereas, Yamada and Suzuki⁵ have recently shown that for coherent tunneling, the tunneling conductance of a d -wave SIS junction is distinctly different when compared to incoherent tunneling. The subgap region of the coherent SIS tunneling conductance is almost linear in V . They find that the quasiparticle tunneling in a Bi2212 mesa is mostly coherent. In general, the symmetry and pairing mechanism of the superconducting state remains controversial. For this reason, it is important to measure the subgap tunneling DOS of SIS Bi2212 junctions at very low temperatures and at high magnetic fields. While the results of measurements of the superconducting energy gap in SIS junctions are insensitive to thermal broadening, measurement in the mK region are required to rule out thermal excitations as the origin of both the excess conductance at zero voltage and the broadening of the conductance peak.

Magnetic field is essential, first, in order to suppress the Josephson current, which makes the measurement of the subgap tunneling conductance difficult. Secondly, the magnetic field is very useful to distinguish relevant information in tunneling data from anomalous features due to critical current effects in weak links of the junction and the Bi2212 single crystal. Finally, it is necessary to study the effect of the magnetic field on the subgap and gap structures in the tunneling spectra.

Over the past few years the local DOS in Bi2212 has often been studied spectroscopically using a scanning tunneling microscope (STM). During the process of the mechanical cleaning, the crystal breaks between the BiO planes of two adjacent half-unit cells.⁶ In the case of tunneling measurements performed on the BiO plane, the large separation between the tip and the pair of CuO_2 planes (greater than 10 Å) precludes the possibility of tunneling directly into these planes. In this situation, the electronic states of planes other than CuO_2 play a role in the tunneling process and must be taken into account.⁷ In contrast to STM, in a break junction fabricated on Bi2212 single crystals by using a precision setup, the tunneling can occur along CuO_2 planes because many plane edges are created. It should be pointed out that since Bi2212 single crystals can be easily cleaved, the pos-

sibility exists that the crystal shears along a plane rather than breaking cleanly, leading to the formation of a c -axis junction, but we will argue later that the tunneling in our break junctions is most likely to be in the ab plane. There are a number of articles that have shown that a mechanically controllable break junction is one of the better tunnel systems (see, e.g., Refs. 3, 8, and 9). Breaking the crystal at cryogenic temperatures and in high vacuum (or in an inert cryogenic fluid) guarantees two atomically clean surfaces, thereby minimizing surface contamination. The distance between these surfaces can be mechanically controlled. Increasing the distance results in a smaller junction, which is eventually reduced to only a few atoms. It is possible to form a tunnel junction with a vacuum barrier between the two foremost atoms.⁹ Although, in view of the technical complexity, this method has not been extensively applied, it has provided reliable results so far, especially in the case of Bi2212 single crystals. At the present time this is the only method which allows a tunneling investigations of Bi2212 single crystals at ultralow temperatures. In this paper we describe an experimental study of the tunneling DOS in copper oxide HTS at temperatures 30–50 mK in high magnetic fields up to 26 T using high-quality break junctions fabricated on Bi2212 single crystals. These investigations are an extension of our previous tunneling studies of the Bi-compound HTS.^{10,11}

II. EXPERIMENT

The Bi2212 single crystals were grown by a KCl-solution-melt-free growth method.^{11,12} It is known that overdoping or underdoping of Bi2212 can be achieved by changes in the oxygen content or by cation substitutions.^{13,14} The first method requires an annealing in oxygen or argon at very high temperatures. A careful characterization of the annealed samples reveals that changes in T_c are always accompanied by a severe degradation of the sample quality. Kinoda *et al.*¹⁵ have showed also that the annealing in oxygen can substantially increase the gap inhomogeneity. For this reason we have used only high quality *as-grown* single crystals in which the substitution of trivalent Bi for divalent Sr during growth reduces the hole concentration in the CuO_2 planes.¹⁶ As the Bi/Sr ratio increases, the number of holes doped into the system decreases, which therefore pushes the system towards the hole-underdoped regime. Very recently Eisaki *et al.*¹⁷ have shown that as the Bi/Sr ratio in $\text{Bi}_{2+x}\text{Sr}_{2-x}\text{CaCu}_2\text{O}_{8+\delta}$ single crystals approached 1, T_c increases from 82.4 K for $x=0.2$ to 91.4 K for $x=0.07$, 92.6 K for $x=0.04$, and eventually to 94.0 K. Bi2212 single crystals with the excess Bi have repeatedly been used in the tunneling study of temperature and doping dependence of the superconducting gap and pseudogap (see, e.g., Ref. 18).

The quality of the crystals was verified by measurements of the dc resistance, ac susceptibility, x-ray diffraction, and scanning electron microscopy. The single crystal showed x-ray rocking curves with a width of about 0.1° demonstrating the high quality and high homogeneity of the samples. The values of the residual resistivity in our crystals were comparable with the lowest value previously reported for

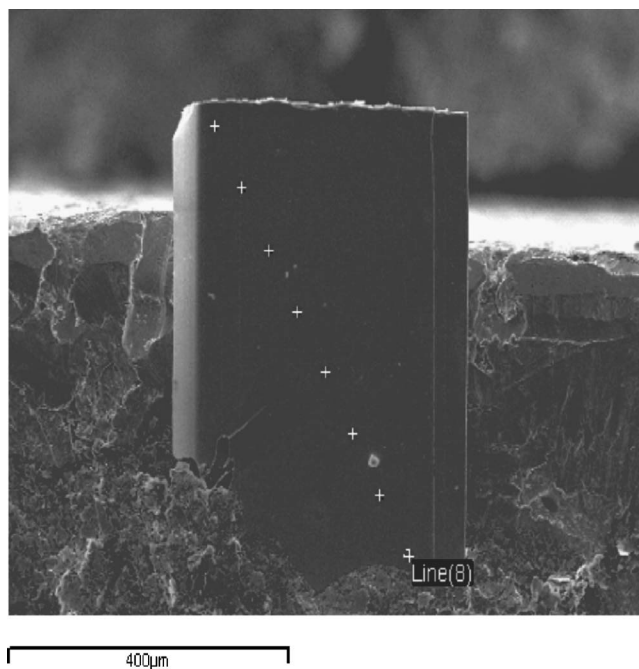


FIG. 1. The scanning electron micrograph of a crystal fragment where the composition measurement points are denoted by crosses.

Bi2212. (see, e.g., Ref. 19). The composition of the crystals was studied using a Philips CM-30 electron microscopy with a Link analytical AN-95S energy dispersion x-ray spectrometer.²⁰ The actual cationic compositions of each crystal investigated were measured at several different places on the crystal and the scatter in the data was less than 2%. In Fig. 1 we show a scanning electron micrograph of a crystal fragment where the composition measurement points are denoted by crosses. Previously, we have measured the Hall coefficient in several crystals and found the nearly linear relation between the excess Bi and the hole concentration p . Our samples showed the well-known parabolic behavior for $T_c(p)$.

Since the deviation from conventional superconductivity should be most pronounced in the underdoped regime, for the present study, we have chosen three underdoped *as-grown* single crystals $\text{Bi}_{2.22}\text{Sr}_{1.55}\text{Ca}_{1.17}\text{Cu}_{2.01}\text{O}_{8+\delta}$ with $T_c=84$ K and transition width $\Delta T_c=1.5$ K. The same hole concentration for the investigated samples $p=0.125$ has been obtained from the Bi/Sr ratio as well as from the empirical relation $T_c/T_{c,max}=1-82.6(p-0.16)^2$ which is satisfied for a number of the HTS.²¹ We used the fact that the substitution of trivalent Bi for divalent Sr in the Bi compounds reduces the hole concentration in the CuO_2 planes.¹⁶

In order to demonstrate that the investigated samples are underdoped, in Fig. 2 we show the temperature dependence of the in-plane resistivity ρ_{ab} for one of the investigating crystals (#1, $p=0.125$). For comparison, we show also $\rho_{ab}(T)$ for the overdoped ($p=0.2$) single crystal with the same $T_c=84$ K (midpoint) as well as the data for the slightly underdoped sample with $T_c=87$ K ($p=0.13$). One can see that as in all Bi compound HTS, the magnitude of $\rho_{ab}(T)$ increases with decreasing carrier concentration. A typical T -linear behavior and a slightly upward curvature of ρ_{ab} are

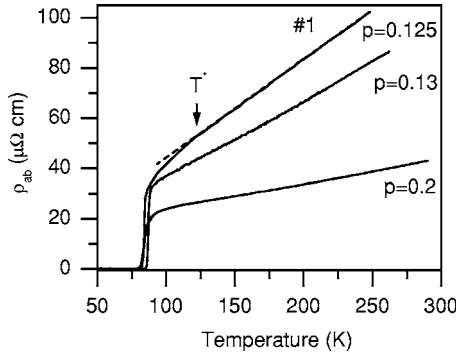


FIG. 2. The temperature dependence of the in-plane resistivity ρ_{ab} for one of the investigating underdoped crystals (#1, $p=0.125$). For comparison, we show also $\rho_{ab}(T)$ for an overdoped ($p=0.2$) single crystal with the same $T_c=84$ K (midpoint) as well as the data for a slightly underdoped sample with $T_c=87$ K ($p=0.13$).

also seen in the slightly underdoped and the overdoped samples. Whereas for the underdoped sample ($p=0.125$), ρ_{ab} deviates from high-temperature T -linear behavior at a characteristic temperature T^* (indicated by the arrow in Fig. 2), as would be expected. This temperature in Ref. 22 was identified as the pseudogap closing (opening) temperature T^* . This is a further proof that we are measuring truly underdoped samples.

The dimensions of the investigated crystals were $\approx 1 \text{ mm} \times (0.5-1) \text{ mm} \times (1-3) \mu\text{m}$. A four-probe contact configuration, with symmetrical positions of the low-resistance contacts ($< 1 \Omega$) on both ab surfaces of the sample was used. For the tunneling measurements, the sample was cooled to 30 mK at zero magnetic field. The tunnel junction was then fabricated *in situ* using a mechanical break-junction technique. With the geometry of the setup used, the break junctions forms so that tunneling occurs in the ab plane. The $I(V)$ characteristics and differential conductances dI/dV as functions of V were measured using phase-sensitive detection techniques. We were able to fabricate a large number of tunnel break junctions at different places along the initial break with resistances from 100 Ω to 120 $k\Omega$ (for bias voltages around 300 mV). Each junction was stable with reproducible characteristics at different magnetic fields. With our break-junction setup the magnetic field was oriented parallel to the CuO_2 planes to an estimated accuracy of $\approx 1^\circ$.¹⁰

In a previous investigation we have measured break-junction tunneling together with the ab -plane and out-of-plane resistivities for the same Bi2212 crystal at different temperatures (4.2–250 K) for magnetic fields up to 20 T oriented parallel to the c axis.¹⁰ In a magnetic field $\rho_{ab}(T)$ reveals a significant increase in the width of the superconducting transition, while the value T_c for the onset of superconductivity remained constant. The data for $\rho_c(T)$ show evidence for a strong suppression of the superconductivity along the c axis in a magnetic field of 20 T. The observed decrease of the T_c value by a factor 2 indicates a significant reduction of the energy gap. In contrast, for all tunnel junctions investigated the energy gap is almost independent of the magnetic field ($H \parallel c$ axis) ≤ 20 T.¹⁰ For this

reason, we can formally state that the observed gap spectrum for our break junctions is related to the ab plane superconducting energy gap and therefore to tunneling in the ab plane. At the same time, we are unable to say anything about the tunneling direction in the ab plane itself. For example, it was shown in Ref. 23 that the shape of spectra measured using point contact tunneling spectroscopy of $\text{YBa}_2\text{Cu}_3\text{O}_7$ within the ab plane in the [100] and [110] directions were quite different, although the extracted magnitudes of the energy gap were in close agreement. The exact knowledge of the tunneling direction is essential for point contact tunneling spectroscopy where the main contribution to the quasiparticle current is given by Andreev reflection, which strongly depends on the wave vector. However, this is not the case for tunnel junctions. Hoogenboom *et al.*² have shown on the basis of a detailed analysis of a large number of tunneling and ARPES spectra that the tunneling spectroscopy probes states along the entire Fermi surface.

III. BREAK-JUNCTION TUNNELING SPECTROSCOPY

Figures 3(a)–3(c) shows representative $I(V)$ curves together with the tunneling conductances data $dI/dV(V)$ for a 100 Ω -, 115 $k\Omega$ -, and a 6 $k\Omega$ tunnel junction, respectively, at $T \approx 40$ mK, for different magnetic fields (sample #1). All the $I(V)$ characteristics exhibit characteristic features typical for superconducting tunnel junctions, with a flat region around zero bias, consistent with the expected zero tunneling conductance [the insets in Figs. 3(a)–3(c)], and a well-defined sharp increase in the tunnel current near $\pm(45-65)$ mV connected with the superconducting gap. At large bias voltages up to ± 0.6 V, the $I(V)$ characteristics are linear with small deviation (increasing conductance) as expected for junctions with a good tunnel barrier without current leakage.²⁴ The $I(V)$ characteristics for the low-resistance tunnel junction in the subgap region [Fig. 3(a)] are also typical for low-resistance Josephson junctions (the arrows indicate the direction of the bias current sweep during the measurements). The $I(V)$ curves of this type were hysteretic (versus bias sweep direction) and have the slope of this switching. This is evident even from Fig. 3(a). In accordance with the direction of the bias current sweep, the Josephson current in zero magnetic field equals -76 and $+120 \mu\text{A}$. In our Bi2212 break junctions we have observed the expected Fraunhofer-like dependence of the Josephson critical current as a function of magnetic field. The large period of Fraunhofer pattern points to the excessively small size of the tunnel junctions. After the suppression of the Josephson current in a magnetic field, the tunneling conductances $dI/dV(V)$ of these junctions have a well-defined large zero-flat region around zero-bias voltage [the lower inset in Fig. 3(a)]. The high-resistance junctions do not show a zero-bias peak even at $H=0$ T.

It should be pointed out that Joule heating effects could be important at the ultralow temperatures, especially for low impedance junctions. Previously we have studied Joule heating effects in break junctions fabricated on Bi2212 (Ref. 10) and $\text{Bi}_2\text{Sr}_2\text{CuO}_{6+\delta}$ (Bi2201) (Ref. 25) single crystals. It was found that the shape of the tunneling conductance $dI/dV(V)$

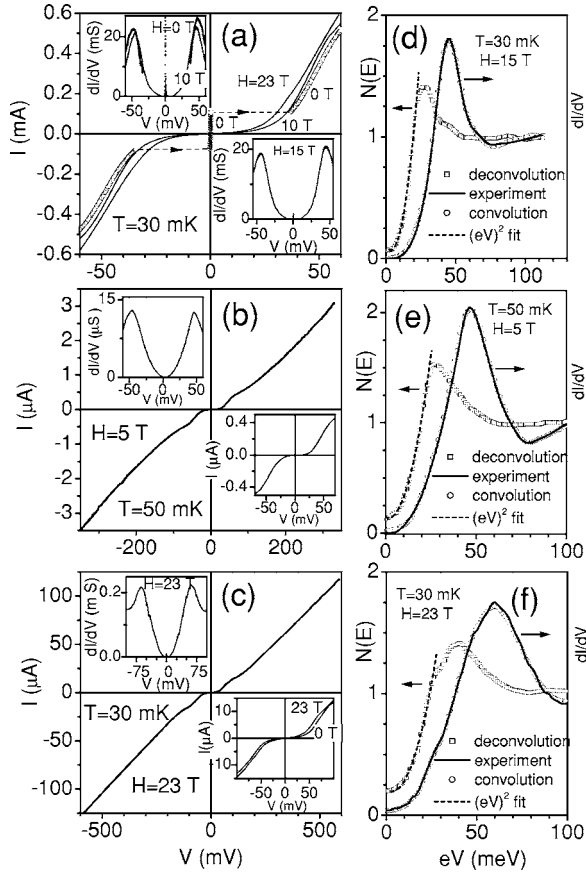


FIG. 3. $I(V)$ characteristics for the (a) 100 Ω -, (b) 115 k Ω -, and (c) 6 k Ω -resistance tunnel junctions at $T=30$ and 50 mK, in different magnetic fields (sample #1). The insets in (a) and the upper insets in (b) and (c) show the corresponding tunneling conductances data $dI/dV(V)$ in the subgap region. The lower insets in (b) and (c) show the same $I(V)$ characteristics in the gap region. (d)–(f) the data points (squares) represent the density of states $N(E)$ obtained from the deconvolution of Eq. (1) (see text).

and the value of the zero-bias dI/dV are very sensitive to a heating of the crystal region near the tunnel barrier. The $dI/dV(V)$ characteristics in our data [Figs. 3(a)–3(c)] show no evidence whatsoever of heating. The linearity of the current-voltage characteristics at high bias voltages (up to 0.6 V) indicates that the heating caused by the current injection in our measurements is negligible. The shape of the tunneling conductance $dI/dV(V)$ is unchanged despite a variation in the junction resistance of three orders of magnitude.

The measured tunneling conductances in the subgap region at $|V| > 10$ mV can be fitted quite well to curves which are quadratic in V . The tunneling conductances in the case of the high-resistance tunnel junctions in Figs. 3(b) and 3(c) in the subgap region do not show a large zero flat region. We have similar characteristics to those shown in Figs. 3(a)–3(c) for several tens of tunnel break junctions formed on each of the three single crystals. We have never observed either a linear increase of the tunneling conductances with voltage in the subgap region, or a nonzero zero-bias conductance for temperatures ≈ 50 mK. The conductance spectra with a flat

bottom seem at first sight to be consistent with s -wave rather than d -wave superconductivity. It should be pointed out that the nonlinear subgap tunneling conductance in the vicinity of the zero bias has been observed previously in Bi2212 (Refs. 8 and 10) and Hg-based cuprates^{26,27} at 4.2 K, but the magnitudes of the background conductances at zero voltage were sizable, suggesting a significant density of states of quasiparticles at zero energy.

Our results are nevertheless puzzling since the tunneling conductances in the subgap region in s -wave SIS junctions at mK temperatures should have the zero flat region practically up to the gap voltages $\pm 2\Delta/e$, and exhibit a very sharp conductance peak structure at $V = \pm 2\Delta/e$. This is clearly not in agreement with our results. Despite the fact that the measurements were carried out at very low temperatures, the gap structure is strongly smeared with a broad conductance peak, and the shape of the tunneling spectra are not consistent with the expected tunneling conductance for s -wave superconductors at temperatures near 0 K. On the other hand, the quadratic in V behavior of the subgap tunneling conductances observed in this work is in agreement with the conductance of the SIS junction calculated by Won and Maki⁴ with d -wave order parameter, although the shape of our experimental curves at voltages above the conductance peaks differs strongly from the theoretical curves.

IV. QUASIPARTICLE DENSITY OF STATES

In order to extract the quasiparticle DOS, $N(E)$, from the tunneling conductances in Figs. 3(a)–3(c), we deconvoluted the expression for the normalized tunneling conductance²⁴

$$\frac{dI/dV(V)_S}{dI/dV(V)_N} = \frac{d}{d(eV)} \int_0^{eV} N(E)N(E-eV)dE. \quad (1)$$

This expression suggests that a tunneling matrix element which weights a particular momentum direction is a constant and the tunneling spectrum directly relates to the DOS in the CuO₂ plane. Although in some articles the tunneling spectrum was considered to be suggestive of an anisotropic matrix element, in Ref. 2 it was shown on the basis of a detailed analysis of the tunneling and angle-resolved photoemission spectroscopy (ARPES) spectra that the tunneling matrix element does not have a strong dependence on the wave vector. Tunneling spectroscopy therefore equally probes states over the entire Fermi surface.²

An iterative procedure for the deconvolution together with the method used to obtain the normalized tunneling conductance is described in Ref. 10. In Figs. 3(d)–3(f) the data points (squares) represent the result of this deconvolution for three different tunneling junctions from Figs. 3(a)–3(c), respectively. The solid lines show the experimental conductance curves $(dI/dV)_S/(dI/dV)_N$ compared with the calculated curves (circles) using the $N(E)$ obtained from

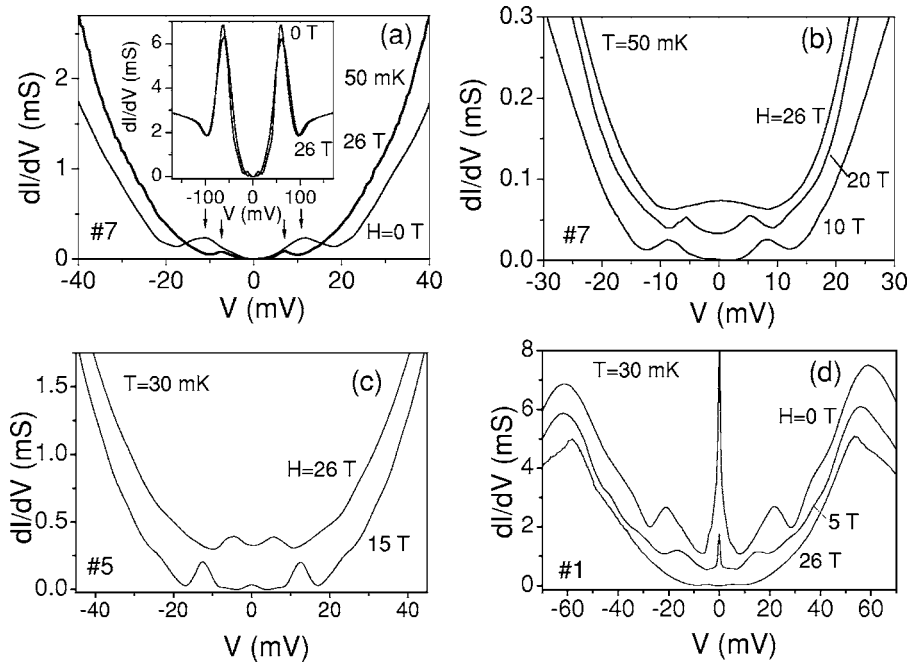


FIG. 4. The effect of the magnetic field on the gaplike structure (marked by arrows) in the tunneling conductance dI/dV vs V within the superconducting gap for different break junctions on three single crystals at $T=50$ mK and $T=30$ mK. (a) and (b) two tunnel break junctions with resistance nearly 1 k Ω fabricated with the same single crystal #7. The inset shows the full gap spectra at 0 and 26 T. (c) and (d) the subgap regions of the spectra on an enlarged scale for two single crystals #5 and #1 (the resistances nearly 300 Ω). For clarity, the curves in (b)–(d) have been shifted vertically with respect to the lower curves.

the deconvolution of Eq. (1). The good agreement with the data in Figs. 3(d)–3(f) confirms the validity of the iterative procedure used to obtain $N(E)$. The shape of the $N(E)$ showed in Figs. 3(d)–3(f) is fully compatible with a smeared BCS DOS for Bi2212.¹⁰ The obtained $N(E)$ over the entire subgap region can be fitted quite well to curves which are quadratic in V (dashed lines). A quadratic rather than linear increase of $N(E)$ in the subgap region seems to be strong evidence against d -wave symmetry.

Note that a quadratic or nonlinear voltage dependence of the subgap tunneling conductance in Bi2212 has been observed previously in STM experiments, for example in Refs. 7, 28, and 29. Franz and Millis³⁰ have shown that a reasonable fit to the data in Ref. 29 assuming a DOS with a d -wave order parameter could be made provided the tunneling matrix element is anisotropic. Assuming an isotropic (constant) matrix element leads to a sharper V -shaped gap structure, inconsistent with the experimental data.²⁹ As previously noted, the tunneling matrix element is most likely independent of the wave vector,² which implies that the STM spectra give the quasiparticle DOS directly, and are, therefore, inconsistent with a pure d -wave order parameter, in agreement with our results. For this reason, we are forced to conclude that it is not possible to explain our data in terms of either pure s pairing or pure $d_{x^2-y^2}$ pairing. Our results lead to the conclusion that Bi2212, in all likelihood, has a $d+s$ mixed pair state, as has been repeatedly suggested in the literature (see, e.g., Refs. 31 and 32).

V. SUBGAP STRUCTURE

In addition, a large number of the tunnel break junctions exhibited $dI/dV(V)$ curves with gaplike features within the gap at voltages ~ 6 – 20 mV. With increasing magnetic field

this structure broadens, diminishes in amplitude, and shifts to lower voltages. In Fig. 4, we show the subgap regions of the differential conductances dI/dV as a function of the bias voltage V in different magnetic fields at $T \approx 50$ mK. (a) and (b)—two tunnel break junctions with a resistance of nearly 1 k Ω fabricated with the same single crystal #7 (the low-voltage gaplike structure is indicated by arrows). The inset in (a) shows the full gap spectra at 0 and 26 T in order to compare the amplitude of the subgap features with the gap peak. Figs. 4(c) and 4(d) show the subgap regions of the spectra on an enlarged scale for two single crystals #5 and #1 (with resistances of around 300 Ω). For clarity, the curves in Figs. 4(b)–4(d) have been shifted vertically with respect to the lower curves.

It might be thought that the observed subgap structure are low-energy features related to the zero-bias peak which is caused by d -wave Andreev bound states^{33,34} or the Josephson effect. However, in the case of the higher-resistance break junction [Fig. 4(a)] the zero-bias peak is lacking at $H=0$ T. Nevertheless, both the subgap structure and its field dependence are seen. In Figs. 4(b)–4(d), the subgap–gaplike structure is also clearly visible despite the fact that the zero-bias peak is suppressed completely by the magnetic field. These data show that the zero-bias peak and the subgap–gaplike structure in our case have distinctly different origins.

Taking into account the magnetic field dependence of the gaplike structure observed here, we identify this feature with a small energy gap, the average magnitude of which is $2\Delta_{p-p}^s/e=13$ mV. Electronic structure calculations for Bi2212 have long predicted the presence of BiO-derived bands and a splitting of CuO_2 bands at the Fermi energy. If we assume that the break-junction tunneling averages the DOS equally around the Fermi surface,² then the observed tunneling conductance must involve two separate order parameters derived from different bands. While the subgap structure might be connected with a proximity induced en-

ergy gap in the BiO layers,³⁵ the possible existence of a second small gap ($2\Delta \leq 8-20$ meV) in Bi2212 has been previously suggested by Shen *et al.*,³⁶ Mahan³⁷ and Mallet *et al.*³⁸ in order to explain the gap anisotropy observed in ARPES and vacuum tunneling spectroscopy of Bi2212. It should be pointed out that the weak subgap structure in Bi2212 has been occasionally seen in the vicinity of the zero bias in STM spectra at 4.2 K (Refs. 29 and 39) and break junctions at 10 K.²⁸ It is also possible that the subgap structure detected by us at mK temperatures can manifest itself as a “linear” increase in the subgap region in the vicinity of the zero bias as often observed in the STM spectra of Bi2212 measured at $T=4.2$ K.

VI. SUPERCONDUCTING ENERGY GAP

We now turn our attention to the magnitude of the superconducting energy gap in the studied crystals. For the SIS junctions studied here, the peak-to-peak separation of the two main maxima of the $dI/dV(V)$ curves must correspond to $4\Delta_{p-p}/e$. As can be seen in Figs. 3(a)–3(c), this value is different for the different break junctions formed using the same single crystal (#1) and equals 96, 93, and 124 mV. The applied magnetic field $H\parallel ab$ plane should decrease only slightly the peak-to-peak separation in $dI/dV(V)$ curves due to the very high parallel critical magnetic field in Bi2212. For sample #1, we find a surprisingly wide scatter of the size of the energy gap $2\Delta_{p-p}/e$ ranging from 46 to 78 mV for the more than 50 different break junctions investigated. Similarly, for two other single crystals (#5 and #7), we obtained $2\Delta_{p-p}/e=50-65$ mV and $2\Delta_{p-p}/e=48-72$ mV, respectively.

Miyakawa *et al.*^{28,40} have found a strong monotonic dependence of the superconducting energy gap of the Bi2212 on the doping concentration. However, we can formally exclude macroscopic sample inhomogeneity, as the origin of the observed variation, since $2\Delta_{p-p}/e=46-78$ mV would imply⁴⁰ a spread of hole concentration $p=0.2-0.15$. Using the empirical relation for T_c vs p , this would imply values of T_c ranging from 80 to 95 K. In addition, the chemical composition of the crystal, measured at several different points, is found to be identical (Fig. 1). The crystal is of a very high quality judging from the sharp superconducting transition width $\Delta T_c=1.5$ K (in the magnetization measurements), and the small rocking curve width $\delta\theta \approx 0.1^\circ$. Following Ref. 15, this strongly suggests that such a wide range of the gap values originates from the presence of different superconducting regions on the scale of a few coherence lengths. The effects of a nanoscale chemical inhomogeneity on T_c of Bi2212 was recently studied in Ref. 17. If the sample has a nanoscale disorder with multiple energy gaps, the convolution of several DOS gives a strongly smeared single conductance peak [Figs. 3(a)–3(c)], nevertheless, the DOS after the deconvolution of the conductance can show an additional maximum in the peak region [Fig. 3(f)]. In individual cases the break junctions can show double peaks in the conductance at voltages nearly $2\Delta_{p-p}/e$ (Fig. 5), that is indicative of two nanoscale superconducting regions in the region of the junction.

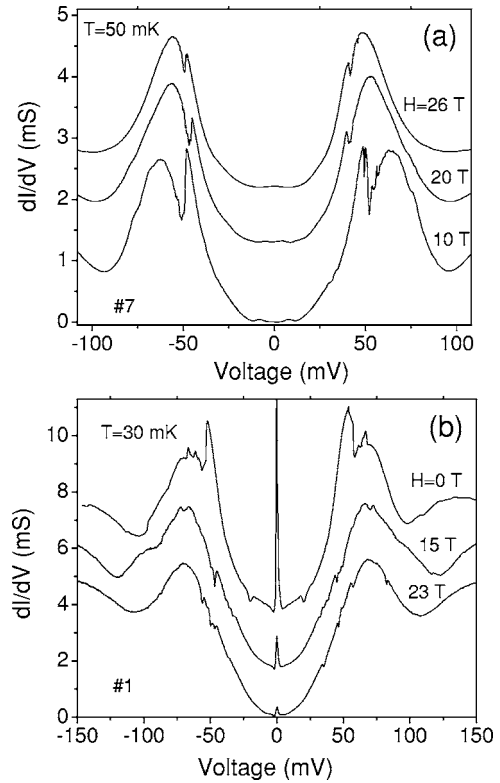


FIG. 5. Differential conductances dI/dV as a function of the bias voltage V for tunnel break junctions fabricated on single crystals #7 and #1 with double peaks in different magnetic fields at $T \approx 50$ mK. For clarity, the curves have been shifted vertically with respect to the lower curves.

VII. CONCLUSION

In conclusion, we have studied the tunneling density of states using high-quality break junctions fabricated on Bi2212 single crystals. Our experiments provide a crucial test for the presence of excitations within the superconducting energy gap. The measured tunneling conductances in the subgap region show a zero flat region. We have never observed either a linear increase of the tunneling conductances with voltage in a subgap region or a nonzero zero-bias conductance at temperatures 30–50 mK. The deconvoluted DOS in the whole subgap region can be fitted quite well to curves which are quadratic in V . A quadratic rather than linear increase of $N(E)$ in the subgap region seems to be strong evidence against pure $d_{x^2-y^2}$ symmetry. The major part of the tunnel break junctions exhibited $dI/dV(V)$ curves with the second energy gap structure with an average magnitude $2\Delta_{p-p}/e=13$ mV. We cannot explain our data with either pure s pairing or pure d pairing. The wide range of the superconducting gap values observed suggests that the results of investigations of the doping dependence of the superconducting gap in HTS by tunneling spectroscopy need to be treated with care.

ACKNOWLEDGMENT

This work has been partially supported by NATO Grant PST.CLG. 979896.

- ¹K. Kitazawa, *Science* **271**, 313 (1996).
- ²B. W. Hoogenboom, C. Berthod, M. Peter, O. Fischer, and A. A. Kordyuk, *Phys. Rev. B* **67**, 224502 (2003), and references cited therein.
- ³J.-F. Zasadzinski, L. Ozyuzer, N. Miyakawa, K. E. Gray, D. G. Hinks, and C. Kendziora, *Phys. Rev. Lett.* **87**, 067005 (2001).
- ⁴H. Won and K. Maki, *Phys. Rev. B* **49**, 1397 (1994).
- ⁵Y. Yamada and M. Suzuki, *Phys. Rev. B* **66**, 132507 (2002), and references cited therein.
- ⁶P. A. P. Lindberg, Z. X. Shen, B. O. Wells, D. S. Dessau, D. B. Mitzi, I. Lindau, W. E. Spicer, and A. Kapitulnik, *Phys. Rev. B* **39**, 2890 (1989).
- ⁷S. Misra, S. Oh, D. J. Hornbaker, T. DiLuccio, J. N. Eckstein, and A. Yazdani, *Phys. Rev. Lett.* **89**, 087002 (2002).
- ⁸D. Mandrus, J. Hartge, C. Kendziora, L. Mihaly, and L. Forro, *Europhys. Lett.* **22**, 199 (1993).
- ⁹N. van der Post, E. T. Peters, I. K. Yanson, and J. M. van Ruitenbeek, *Phys. Rev. Lett.* **73**, 2611 (1994).
- ¹⁰S. I. Vedeneev, A. G. M. Jansen, P. Samuely, V. A. Stepanov, A. A. Tsvetkov, and P. Wyder, *Phys. Rev. B* **49**, 9823 (1994).
- ¹¹S. Vedeneev, A. Jansen, and P. Wyder, *Physica B* **300**, 38 (2001) (review article).
- ¹²J. Gorina, G. Kaljuzhnaia, V. Ktitorov, V. P. Martovitsky, V. Rodin, V. Stepanov, A. Tsvetkov, and S. I. Vedeneev, *Solid State Commun.* **85**, 695 (1993).
- ¹³G. Villard, D. Pelloquin, and A. Maignan, *Phys. Rev. B* **58**, 15 231 (1998).
- ¹⁴S. Ooi, T. Shibauchi, and T. Tamegai, *Physica C* **302**, 339 (1998).
- ¹⁵G. Kinoda, T. Hasegawa, S. Nakao, T. Hanaguri, K. Kitazawa, K. Shimizu, J. Shimoyama, and K. Kishio, *Phys. Rev. B* **67**, 224509 (2003).
- ¹⁶J. Harris, P. White, Z.-X. Shen, H. Ikeda, R. Yoshizaki, H. Eisaki, S. Uchida, W. Si, J. Xiong, Z.-X. Zhao *et al.*, *Phys. Rev. Lett.* **79**, 143 (1997).
- ¹⁷H. Eisaki, N. Kaneko, D. L. Feng, A. Damascelli, P. K. Mang, K. M. Shen, Z.-X. Shen, and M. Greven, *Phys. Rev. B* **69**, 064512 (2004).
- ¹⁸A. Matsuda, S. Sugita, and T. Watanabe, *Phys. Rev. B* **60**, 1377 (1999).
- ¹⁹T. Watanabe, T. Fujii, and A. Matsuda, *Phys. Rev. Lett.* **79**, 2113 (1997).
- ²⁰Y. Gorina, G. Kaljuzhnaia, N. Sentyurina, V. Stepanov, and S. Chernook, *Kristallografiya* **50**, 150 (2005) [*Crystallogr. Rep.* **50**, 142 (2005)].
- ²¹J. L. Tallon, J. R. Cooper, P. S. I. P. N. de Silva, G. V. M. Williams, and J. W. Loram, *Phys. Rev. Lett.* **75**, 4114 (1995).
- ²²T. Watanabe, T. Fujii, and A. Matsuda, *Phys. Rev. Lett.* **84**, 5848 (2000).
- ²³J. Y. T. Wei, N.-C. Yeh, D. F. Garrigus, and M. Strasiak, *Phys. Rev. Lett.* **81**, 2542 (1998).
- ²⁴E. Wolf, *Principles of Electron Tunneling Spectroscopy* (Oxford University Press, New York, 1985).
- ²⁵S. I. Vedeneev, P. Szabo, A. G. M. Jansen, and I. S. Vedeneev, *Zh. Eksp. Teor. Fiz.* **119**, 1 (2001) [*JETP* **92**, 851 (2001)].
- ²⁶J. Chen, J. F. Zasadzinski, K. E. Gray, J. L. Wagner, and D. G. Hinks, *Phys. Rev. B* **49**, 3683 (1994).
- ²⁷G. T. Jeong, J. I. Kye, S. H. Chun, S. Lee, S. I. Lee, and Z. G. Khim, *Phys. Rev. B* **49**, 15416 (1994).
- ²⁸N. Miyakawa, J. F. Zasadzinski, L. Ozyuzer, P. Guptasarma, D. G. Hinks, C. Kendziora, and K. E. Gray, *Phys. Rev. Lett.* **83**, 1018 (1999).
- ²⁹C. Renner, B. Revaz, J.-Y. Genoud, K. Kadowaki, and O. Fischer, *Phys. Rev. Lett.* **80**, 149 (1998).
- ³⁰M. Franz and A. J. Millis, *Phys. Rev. B* **58**, 14572 (1998).
- ³¹Q. Li, Y. N. Tsay, M. Suenaga, R. A. Klemm, G. D. Gu, and N. Koshizuka, *Phys. Rev. Lett.* **83**, 4160 (1999), and references cited therein.
- ³²Y. I. Latyshev, A. P. Orlov, A. M. Nikitina, P. Monceau, and R. A. Klemm, *Phys. Rev. B* **70**, 094517 (2004), and references cited therein.
- ³³M. Fogelstrom, D. Rainer, and J. A. Sauls, *Phys. Rev. Lett.* **79**, 281 (1997).
- ³⁴M. Covington, M. Aprili, E. Paraoanu, L. H. Greene, F. Xu, J. Zhu, and C. A. Mirkin, *Phys. Rev. Lett.* **79**, 277 (1997).
- ³⁵A. Yurgens, D. Winkler, N. V. Zavaritsky, and T. Claeson, *Phys. Rev. B* **53**, R8887 (1996).
- ³⁶Z.-X. Shen, D. S. Dessau, B. O. Wells, D. M. King, W. E. Spicer, A. J. Arko, D. Marshall, L. W. Lombardo, A. Kapitulnik, P. Dickinson, S. Doniach, J. DiCarlo, T. Loeser, and C. H. Park, *Phys. Rev. Lett.* **70**, 1553 (1993).
- ³⁷G. D. Mahan, *Phys. Rev. Lett.* **71**, 4277 (1993).
- ³⁸P. Mallet, D. Roditchev, W. Sacks, D. Defourneau, and J. Klein, *Phys. Rev. B* **54**, 13324 (1996).
- ³⁹J. Liu, Y. Li, and C. M. Lieber, *Phys. Rev. B* **49**, 6234 (1994).
- ⁴⁰N. Miyakawa, P. Guptasarma, J. F. Zasadzinski, D. G. Hinks, and K. E. Gray, *Phys. Rev. Lett.* **80**, 157 (1998).